3-1-2019

# Analysis of blade fragment risk at a wind energy facility

Scott Larwood
*University of the Pacific*, slarwood@pacific.edu

David Simms
*National Renewable Energy Laboratory*

Received <day> <Month>, <year>; | Revised <day> <Month>, <year>; | Accepted <day> <Month>, <year>
DOI: xxx/xxxx

**RESEARCH ARTICLE**

# Analysis of blade fragment risk at a wind energy facility

Scott Larwood*[1] | David Simms[2]

[1]Department of Mechanical Engineering, University of the Pacific, California, USA
[2]National Wind Technology Center, National Renewable Energy Laboratory, Colorado, USA

**Correspondence**
*Scott Larwood, Department of Mechanical Engineering, University of the Pacific, Stockton, CA 95211, USA. Email: slarwood@pacific.edu

**Abstract**

An analysis was performed to determine the risk posed by wind turbine fragments on roads and buildings at the National Wind Technology Center at the National Renewable Energy Laboratory. The authors used a previously developed model of fragment trajectory and took into account the wind speed/direction distribution at the site and the probability of rotor failure. The site-specific risk was assessed by determining the likelihood of impact and related consequences. For both the roads and buildings, the risk varied from low to routine, which was considered acceptable.

**KEYWORDS:**
wind energy; hazards; safety

## 1 | INTRODUCTION

At the time of this writing wind energy is the fastest growing source of new energy production. At the end of 2017 (most current year reported (1)), global installed capacity was 539 GW with 89 GW in the United States. US wind energy penetration was at 6.3%; a remarkable achievement considering the amount of total energy production. Although praised for its environmental benefits, wind energy must still be sited with appropriate appreciation for the impact of installations on local land usage. Examples are discussed in Abbasi and Abbasi (2) and in Price et al. (3). This article reports on the potential safety risk posed by wind energy production, which is the possibility of impact of wind turbine blade fragments in the event of structural failure.

Larwood and van Dam (4) reported on the history of this risk and the modeling of rotor fragments in the context of safety setbacks for wind turbines. Since their report, there has been a renewed interest in modeling, with several authors reporting on fragment analysis (5) (6) (7) (8). The state-of-the-art modeling approach is six degrees-of-freedom (6DOF) motion of the blade fragments with aerodynamic loading. Simplified models do not match the results of the 6DOF models; Sørensen (9) showed that drag ballistics do not capture the downwind distance, and the range for vacuum ballistics is too far. All of these models have not been validated with experimental data.

This article presents an analysis of a wind energy facility with several research wind turbines of different sizes. The research site is the National Wind Technology Center (NWTC) which is part of the U.S. Department of Energy's National Renewable Energy Laboratory (NREL). Located south of Boulder, Colorado, the NWTC is nestled at the base of the Rocky Mountain foothills. Researchers have been studying wind energy at the NWTC since the 1970's, originally focusing on small-scale utility turbines. Larger turbines were installed in the 1990's and with the maturity of the industry, multimegawatt turbines, based on production models, have been installed in the past decade. All of the turbines are utilized to support the NWTC's research mission and may be operated outside of conventional parameters. The site is therefore not representative of a typical wind energy plant. The wind season is primarily in the winter with predominant western winds. The site regularly experiences high-velocity foehn winds in the winter (up to 100 miles per hour), making it an ideal location for investigating the reliability and performance of wind turbines.

Eggers et al. (10) reported on a fragment analysis of the NWTC in 2001. Although they made several parametric studies that may pave a path towards generalizing the problem, their overall model assumed a constant drag coefficient ($C_D$) of 0.5, which would be considered high compared to findings from Sørensen (9) and Larwood and van Dam (7). The model was also for a full blade and half-blade thrown from a turbine with a 15.2 m radius on two tower heights (30.4 m and 91.4 m), limited to two wind speeds (11.2 m/s and 22.4 m/s), with a Gaussian distribution of rotor speeds from 1.25 to 1.75 times the rated speed. It is difficult to determine if their results can be scaled to turbines with a higher rating.

The purpose of the study was to analyze the risk posed by rotor fragments from the wind turbines to roads and buildings at the NWTC based on methods developed by Larwood and van Dam (7). The analysis showed that the likelihood of impact with catastrophic consequences to be extremely unlikely, therefore the risk was determined to be low.

## 2 | METHODS

Figure 1 shows a three-dimensional image of the NWTC. The turbines and data sheds of interest are labeled. The roads of interest are the east-west road in green ("main access road") and the northeast-southwest road ("row 4 road") in yellow. CART2 and CART3 are the two-bladed (CART2) and three-bladed (CART3) Controls Advanced Research Turbines.

The purpose of the analysis was to determine the risk of rotor fragments posed by the turbines installed on row 4 on the main entrance road, the row 4 road, and the 4.1, 4.2, and 4.4 data sheds. Table 1 lists details of the turbines that were analyzed.

The analysis requires blade mass properties as inputs. With the exception of the CART turbines, all blade properties were proprietary. Properties were estimated using properties from the WindPACT study (11) and from the modeling described in Larwood et al. (12). The WindPACT models were 1.5 MW and 3 MW, matching the ratings of the GE and Alstom turbines. The blade properties were matched at values of percentage radius. The Siemens turbine was scaled from the 1.5 model using

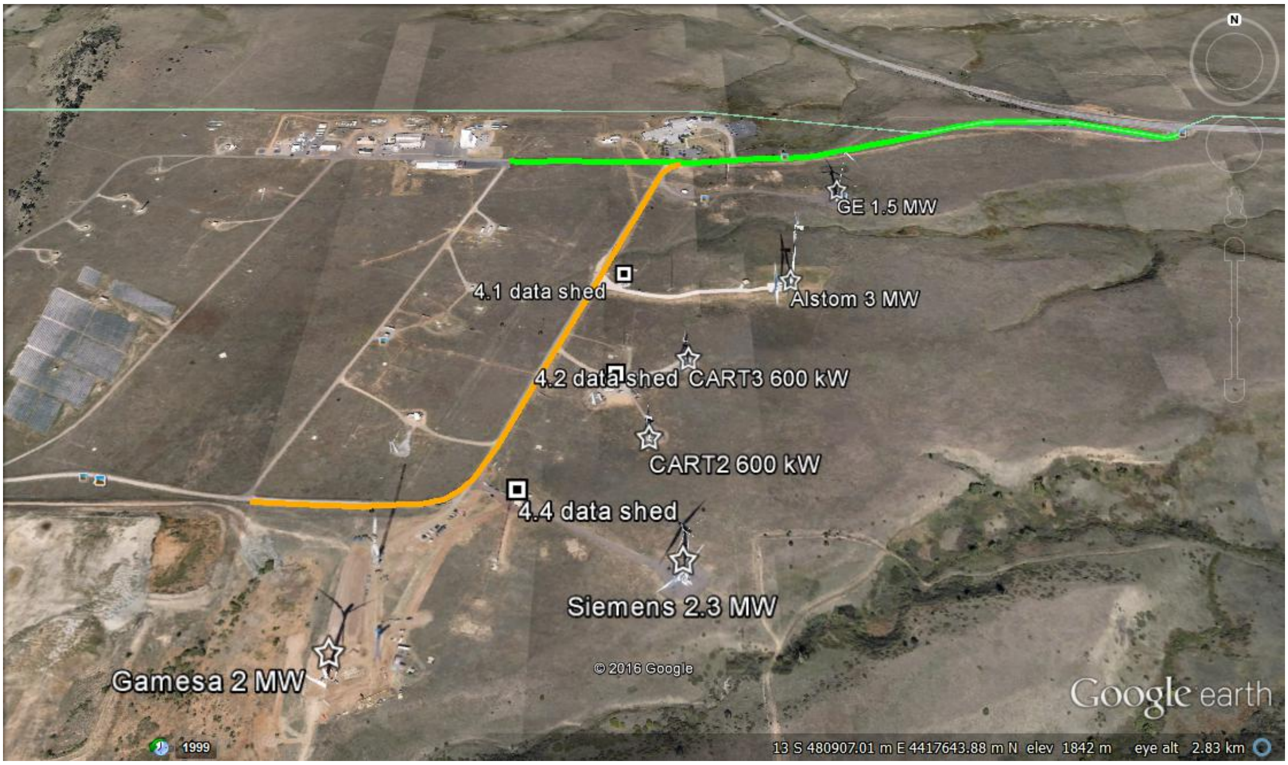


**FIGURE 1** NWTC row 4 wind turbines

**TABLE 1** NWTC turbines

| Turbine | Rating (MW) | Diameter (m) | Hub Height (m) | Rated rpm |
|---|---|---|---|---|
| Alstom ECO 110 | 3 | 110 | 90 | 13.6 |
| CART2 | 0.6 | 42.672 | 36.85 | 41.7 |
| CART3 | 0.6 | 40 | 36.594 | 38 |
| Gamesa G97 | 2 | 97 | 90 | 16 |
| GE 1.5 SLE | 1.5 | 77 | 80 | 18.3 |
| Siemens SWT 2.3 | 2.3 | 106 | 80 | 16 |

scaling laws described in Sarlak and Sørensen (8) for mass, mass center, and mass moment of inertia scaling. The adjustment to the mass was:

$$m = m_{\text{ref}}(r/r_{\text{ref}})^{2.3} \tag{1}$$

where $m_{\text{ref}}$ is the reference (known) mass, and $r_{\text{ref}}$ is the reference radius. The adjustment to the mass center was:

$$d = d_{\text{ref}}(P/P_{\text{ref}})^{1/2} \tag{2}$$

**TABLE 2** Release condition probability

| Input Variable | Probability Distribution |
|---|---|
| Blade pitch | Based on wind speed |
| Rotor rotational speed | Based on wind speed |
| Rotor azimuth at break | Uniform between 0 ° and 360 ° |
| Blade break position | Uniform between hub radius and blade tip |
| Yaw error | Uniform between −10 ° and 10 ° |

where $d_{\mathrm{ref}}$ is the reference (known) distance, and $P_{\mathrm{ref}}$ is the reference rated power. The adjustment to the mass moment of inertia was:

$$I = I_{\mathrm{ref}}(r/r_{\mathrm{ref}})^{4.3} \quad (3)$$

where $I_{\mathrm{ref}}$ is the reference (known) mass moment of inertia. The mass and inertia exponents come from data of actual blade mass versus radius. The diameter is related to the square root of the power. The CART turbine properties were provided by NREL; however, mass center and mass moment of inertia were not available and were therefore scaled from the WindPACT 1.5 model highlighted earlier.

The method used to determine frequency of impact is described in Larwood and van Dam (7). The method models the fragment as a rigid body with translation and rotation. The translation is modeled with Newton's second law and the rotation is determined with Euler's rotation equations. The method also uses equations to determine the changes in the orientation matrix. The fragment is divided into elements to compute the aerodynamic forces using airfoil tables. This method was based on Sørensen (9). The analysis generates 10,000 throws, with release conditions and probability listed in Table 2 . The blade fragment parameters are independent of the wind parameters. The amount of throws was determined by a sensitivity analysis in Larwood and van Dam (7), which showed convergence at 5,000 throws. The wind magnitude and direction are considered random with the probability distribution based on the wind rose, which describes the frequency of occurrence for wind speed and wind direction. The wind rose was from the NWTC M2 meteorological tower (https://www.nrel.gov/midc/nwtc_m2/). Annual wind roses from 2014 and at heights 50 m and 80 m were used (Figure 2 ). Each rose has 8 wind speed distributions for a 30° wind direction sector. The roses show the predominant western wind direction. The CART wind velocities and turbines with 90 m hub height were sheared to hub height with the standard power law as in:

$$V = V_{\mathrm{ref}}(h/h_{\mathrm{ref}})^{\alpha} \quad (4)$$

where $V_{\mathrm{ref}}$ is the reference (known) wind speed, $h_{\mathrm{ref}}$ is the reference height, and $\alpha$ is 1/7. Note that atmospheric turbulence has not been included in the model (was recommended for further study in Ref. (4)).

As an example for a single turbine, Figure 3 shows the impacts for the CART2 at nominal rpm. The impacts are clustered to the south and east of the turbine, which indicates alignment of the turbine with the wind rose.

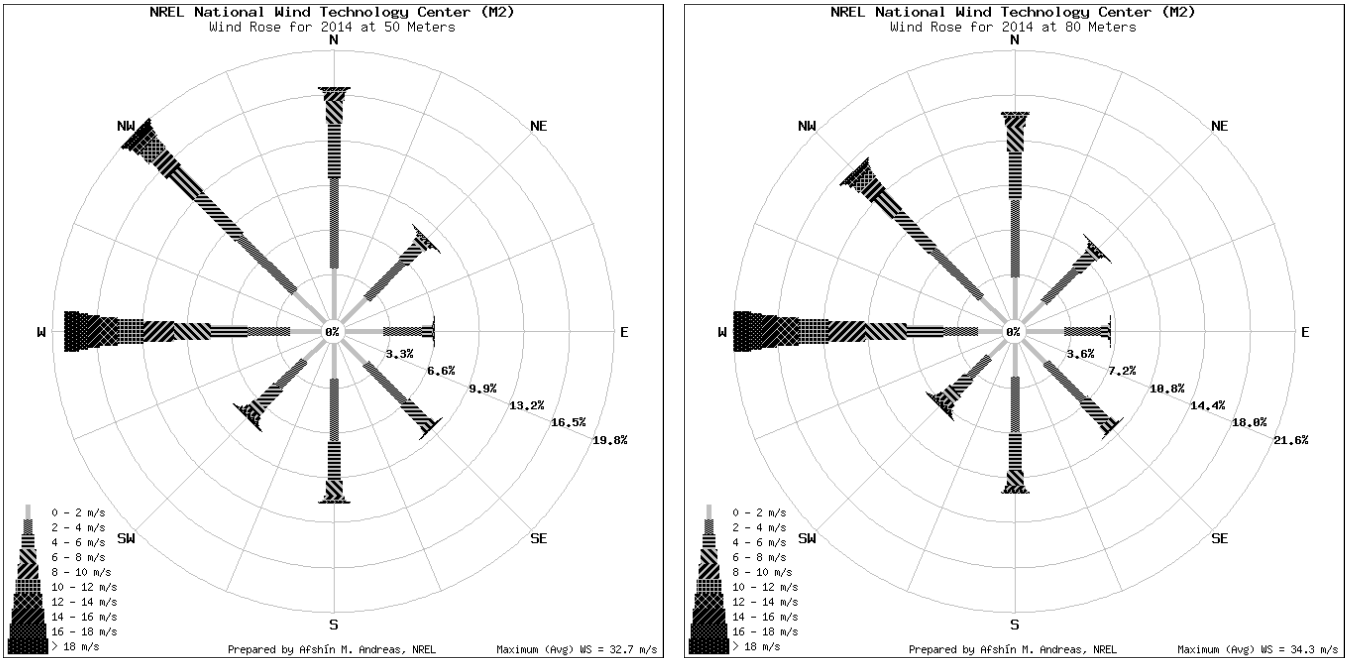


50 m height | 80 m height

**FIGURE 2** NWTC M2 2014 annual wind roses, with circles representing percent of time

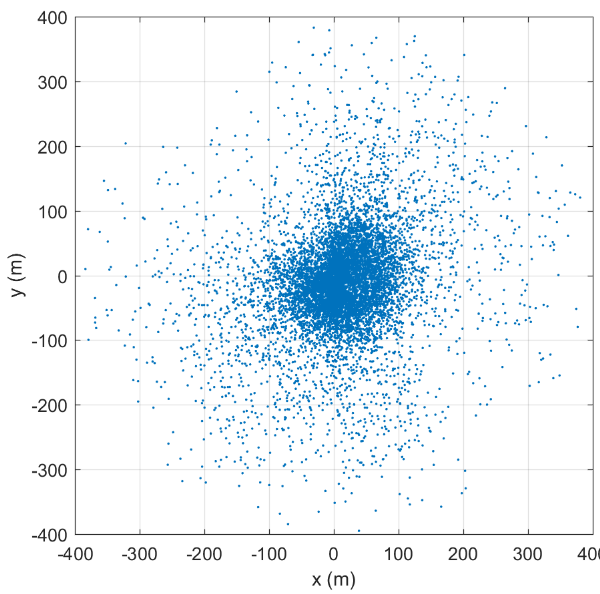


**FIGURE 3** Impacts for CART2 at nominal rpm. East is positive *x* and north is positive *y* in this and following plots.

The probability of impact at a particular ground location is determined by using methods described in Larwood and van Dam (7) and were based on work by Turner (13). The probability of impact from a blade fragment is for a point (used for the roads-impact with vehicle/personnel) and for a target of 25-m-by-25-m-by-3.67-m height (for data sheds). Three separate 10,000 throw

**TABLE 3** Rotor failure probabilities from (14)

| Operating Condition | Probability Per Turbine Per Year |
|---|---|
| Nominal operating rpm | $4.2 \times 10^{-4}$ |
| Braking (1.25 times nominal rpm) | $4.2 \times 10^{-4}$ |
| Emergency (2.0 times nominal rpm) | $5 \times 10^{-6}$ |

**TABLE 4** NREL likelihood values

| Level | Frequency |
|---|---|
| Frequent | $F \geq 1.0/y$ |
| Reasonably Probable | $1.0 > F \geq 0.1/y$ |
| Occasional | $0.1 > F \geq 0.01/y$ |
| Remote | $0.01 > F \geq 10^{-4}/y$ |
| Extremely Remote | $10^{-4} > F \geq 10^{-6}/y$ |
| Improbable | $F < 10^{-6}/y$ |

runs were conducted at rated rpm, braking rpm (1.25 times rated), and emergency rpm (2 times rated). The probability from these runs was multiplied by the failure probability as reported in Braam (14) and listed in Table 3 . Note that these failure data were compiled in 2005. Current failure rates may have decreased with maturity in the technology. However, due to the outcome of this study, no further analysis of failure rates was deemed necessary.

As an example, Figure 4 shows contours (using the MATLAB `contour` function) of constant probability of impact from the CART2 fragments with a point on the ground and for a data shed. For example, the probability of a blade fragment from the CART2 impacting data shed 4.2 is approximately 1 in 10,000, or (0.0001) per year. Again, the alignment of the contours is with the wind rose, with the majority of the impacts occurring perpendicular and downwind from the prevailing wind direction. The uneven contour of the lower probabilities (e.g. 1e-07) is due to a low number of impacts; these contours would be smoother with more throws added to the analysis.

The overall risk was assessed by determining the likelihood and consequence of the impacts. NREL values for likelihood (Table 4 ) and consequence (Table 5 ) were adapted from methods specified in the U.S. Department of Defense Standard Practice for System Safety (15). In the case of the CART2 fragments impacting the 4.2 data shed, the likelihood is considered extremely remote. Note that this example is only for impacts from CART2. The consequence of the impact can vary from negligible to catastrophic depending on several factors including the kinetic energy of the impact and if the shed is occupied at the time of impact. Kinetic energy of the impact can be determined; however, the analysis does not currently include a measure of damage.

The likelihood and consequence are combined into the NREL risk matrix (Figure 5 ) that NREL researchers adapted from methods specified in the U.S. Department of Defense Standard Practice for System Safety (15). NREL considers levels "low" and

**TABLE 5** NREL consequence values

| Level | Consequence |
|---|---|
| Catastrophic | Death; permanent total disability; loss > $10 million |
| Critical | Partial disability; loss > $1 million |
| Marginal | Injury; loss > $100,000 |
| Negligible | Minor injury; loss < $100,000 |

"routine" risk to be acceptable. Fragment impacts with personnel may result in death and therefore are considered catastrophic consequences; however, if the likelihood is extremely remote, the risk is considered low.

## 3 | RESULTS AND DISCUSSION

### 3.1 | Risk Assessment

All throws for the six turbines were combined to determine the overall risk for the site. Figure 6 shows the probability of impact for the roads. The probability is between $1 \times 10^{-5}$ and $1 \times 10^{-6}$ which indicates an "extremely remote" likelihood in Table 4 and a "low" to "routine" risk in Figure 5 . The risk as a result of impact from blade fragments on the roads is therefore considered acceptable.

Figure 7 shows the probability of impact for the sheds. The sheds are very close to the $1 \times 10^{-4}$ probability line, which places the likelihood between "remote" and "extremely remote" in Table 4 . The sheds will, at most, be occupied one-third of a year, which would make the likelihood of injury from blade fragments less than $1 \times 10^{-4}$ $(1/3 \times 1 \times 10^{-4})$ and therefore "extremely remote." Depending on the severity of the injury (consequence), the risk is "low" to "routine" in Figure 5 . Impact from fragments may cause damage to the sheds; however, it would not likely exceed $1 million. Therefore, the damage (consequence) at most will be considered "negligible" to "marginal" in Table 5 . With a "remote" likelihood, the risk for damage to the sheds from blade fragments is "low" to "routine." The risk as a result of impact from blade fragments on the sheds is therefore considered acceptable.

### 3.2 | Comparison with Commercial Plant Analysis

As an extension of this work, the results were compared to setbacks recommended in Larwood and van Dam (7). Row 4 of the NWTC approximates the spacing of a typical wind plant, with 3-rotor-diameter spacing along the row. The exception is the positioning of the two smaller turbines: CART2 and CART3. Row-to-row spacing in wind plants can vary from 5 to 10 diameters; therefore, the probability of impact from other upwind/downwind rows would be negligible at a particular row. Figure 8 shows the probability of point impact (same as Figure 6 for the roads), with circles of radius that are two times the overall height of the turbine. The overall height is defined as the hub height plus the rotor radius. This was a setback proposed by Larwood and van Dam (7) for property line setbacks. For the most part, the probability of impact at this setback is $1 \times 10^{-6}$ and therefore considered "improbable" with a "routine" risk level. The exception to this is the area surrounding the CARTs, which increase the probability of impact upwind of the Siemens turbine (second most southerly turbine).

Figure 9 shows the probability of building impact (same as Figure 7 for the shed), with circles of radius that are three times the overall height of the turbine. This was a setback proposed by Larwood and van Dam (7) for distances to dwellings. The probability of impact is at or above $1 \times 10^{-6}$ and therefore would not result in a "routine" risk level for all consequences. However, moving to 3.5 times the overall height would lower the risk to a "routine" level for all consequences.

## 4 | CONCLUSIONS

An analysis was performed on the risk associated with wind turbine blade fragments from research wind turbines at the National Wind Technology Center at the National Renewable Energy Laboratory. The objective was to demonstrate application of the risk analysis methodology, and does not represent risks associated with commercial wind turbines or plants. The analysis used a previously developed model for the blade fragment trajectory and the associated probability of impact around the turbines. The likelihood and consequences of the impacts were assessed and an overall risk was determined for various roads and structures located in the vicinity of the turbines. The risk was determined to range from "low" to "routine" and was considered acceptable.

As mentioned in previous work, the trajectory model used in this work and other models in the literature could benefit from experimental validation. The study of this hazard would also benefit from an updated investigation of rotor failure probability.

### 4.1 | *Note on retracted version*

This article was previous retracted (16) by agreement between the authors, the journal Editor in Chief, Prof. Simon Watson and John Wiley and Sons Ltd. The retraction was agreed due to an error in the conclusion, which used the analysis of NREL's wind site for evaluation of wind turbine setbacks in general. The assumptions and results do not apply to commercial wind energy sites, as the previous conclusion suggested, and was therefore not suitable for setback recommendations in other locations.

### 4.2 | *Acknowledgements*

The authors would like to thank Lee Jay Fingersh at the NWTC for providing the CART turbine data and some insight into the problem, along with Sheri Anstedt at NREL for editorial assistance.

## References


[1] Wiser Ryan H., Bolinger Mark. *2017 Wind Technologies Market Report*. U.S. Department of Energy; 2018.

[2] Abbasi SA, Abbasi N. The likely adverse environmental impacts of renewable energy sources. *Applied Energy*. 2000;65(1–4):121 - 144.

[3] Price T, Bunn J, Probert D, Hales R. Wind-energy harnessing: Global, national and local considerations. *Applied Energy*. 1996;54(2):103 - 179.

[4] Larwood S, Dam CP. *Permitting Setback Requirements for Wind Turbines in California*. CEC-500-2005-184: California Energy Commission; 2006.

[5] Rogers J, Slegers N, Costello M. A method for defining wind turbine setback standards. *Wind Energy*. 2012;15(2):289-303.

[6] Carbone G, Afferrante L. A novel probabilistic approach to assess the blade throw hazard of wind turbines. *Renewable Energy*. 2013;51:474 - 481.

[7] Larwood S, Dam CP. Wind turbine rotor fragments: impact probability and setback evaluation. *Clean Technologies and Environmental Policy*. 2015;17(2):475-484.

[8] Sarlak H, Sørensen JN. Analysis of throw distances of detached objects from horizontal-axis wind turbines. *Wind Energy*. 2016;19(1):151-166.

[9] Sørensen JN. On the Calculation of Trajectories for Blades Detached from Horizontal Axis Wind Turbines. *Wind Engineering*. 1984;8(3):160-175.

[10] Eggers AJ, Holley WE, Digumarthi R, Chaney K. Exploratory Study of HAWT Blade Throw Risk to Nearby People and Property. In: Migliore P, ed. *2001 ASME Wind Energy Symposium*, AIAA and ASME 2001 (pp. 355-367).

[11] Griffin DA. *WindPACT Turbine Design Scaling Studies Technical Area 1.Composite Blades for 80- to 120-Meter Rotor*. NREL/SR-500-29492: National Renewable Energy Laboratory; 2001.

[12] Larwood S, Dam CP, Schow D. Design Studies of Swept Wind Turbine Blades. *Renewable Energy*. 2014;71:563-571.

[13] Turner DM. An analysis of blade throw from wind turbines. In: Swift-Hook Prof. D.T., ed. *Wind Energy and the Environment*, London: Peter Peregrinus, Ltd. 1989 (pp. 112-135).

[14] Braam H, Mulekom GJ, Smit RW. *Handboek Risicozonering Windturbines*. SenterNovem; 2005.

[15] U.S. Department of Defense . *Department of Defense Standard Practice Safety System*. MIL-STD-882E: Headquarters Air Force Materiel Command; 2012.

[16] Larwood S, Simms D. Retracted: Analysis of blade fragment risk at a wind energy facility. *Wind Energy*. 2018;21(8):681.


**How cite this article:** S. Larwood, D. Simms (TBD), Analysis of blade fragment risk at a wind energy facility, *Wind Energy*, *TBD;TBD:TBD–TBD*.

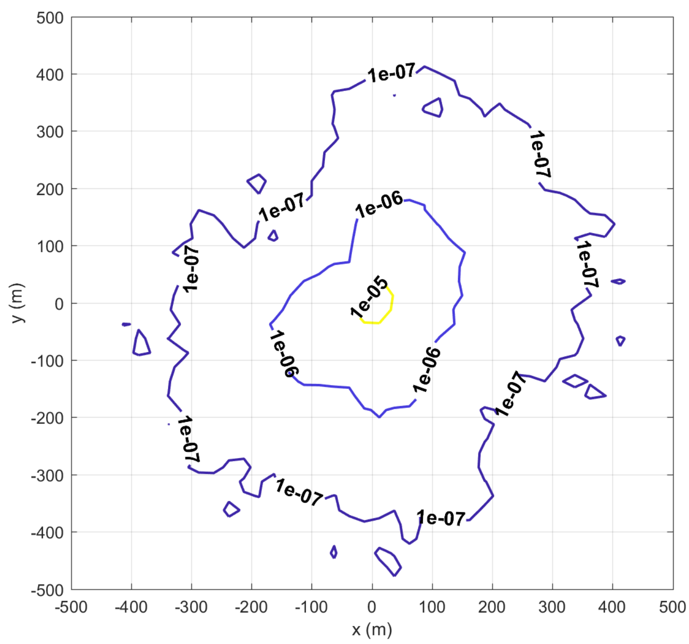


Point impact

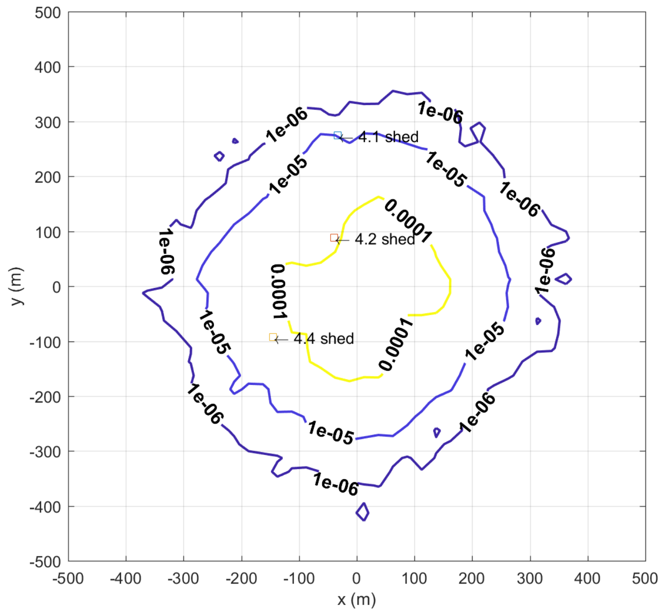


Shed impact

**FIGURE 4** Probability of impact for CART2

Likelihood

Consequence

| | Frequent | Reasonably Probable | Occasional | Remote | Extremely Remote | Improbable |
|---|---|---|---|---|---|---|
| Catastrophic | High | High | High | Moderate | Low | Routine |
| Critical | High | High | Moderate | Low | Low | Routine |
| Marginal | Moderate | Moderate | Low | Low | Routine | Routine |
| Negligible | Routine | Routine | Routine | Routine | Routine | Routine |

**FIGURE 5** NREL risk matrix

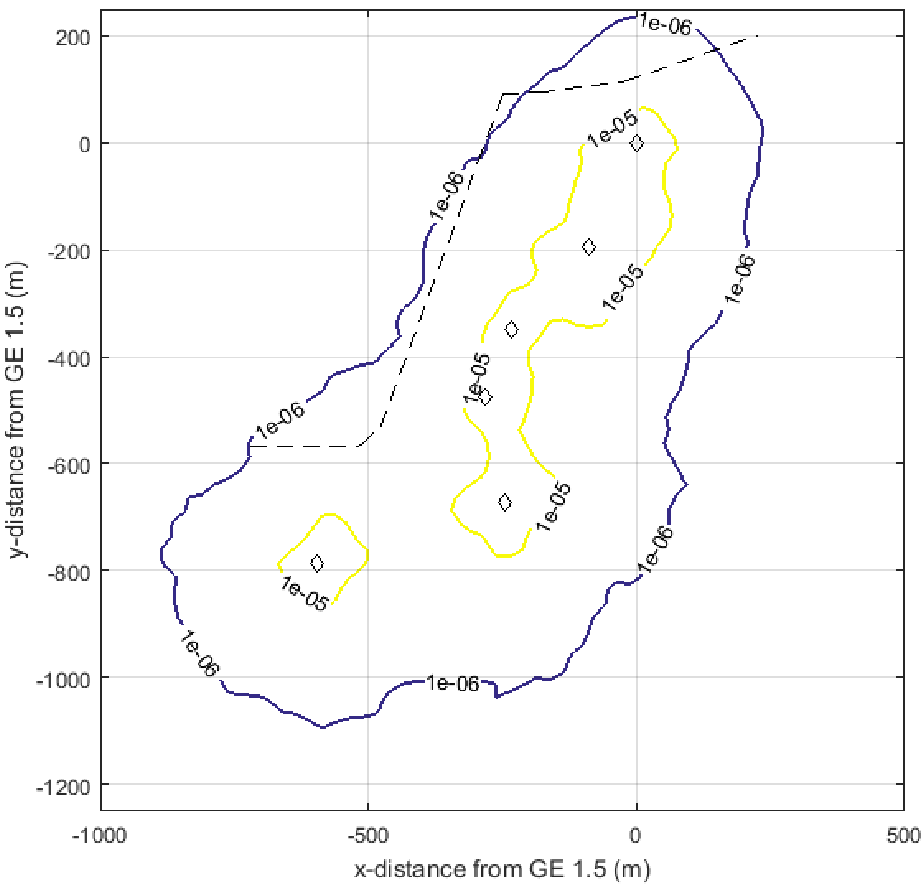


**FIGURE 6** Probability of impact for roads (– – –). Turbines are indicated by open diamonds (◇)

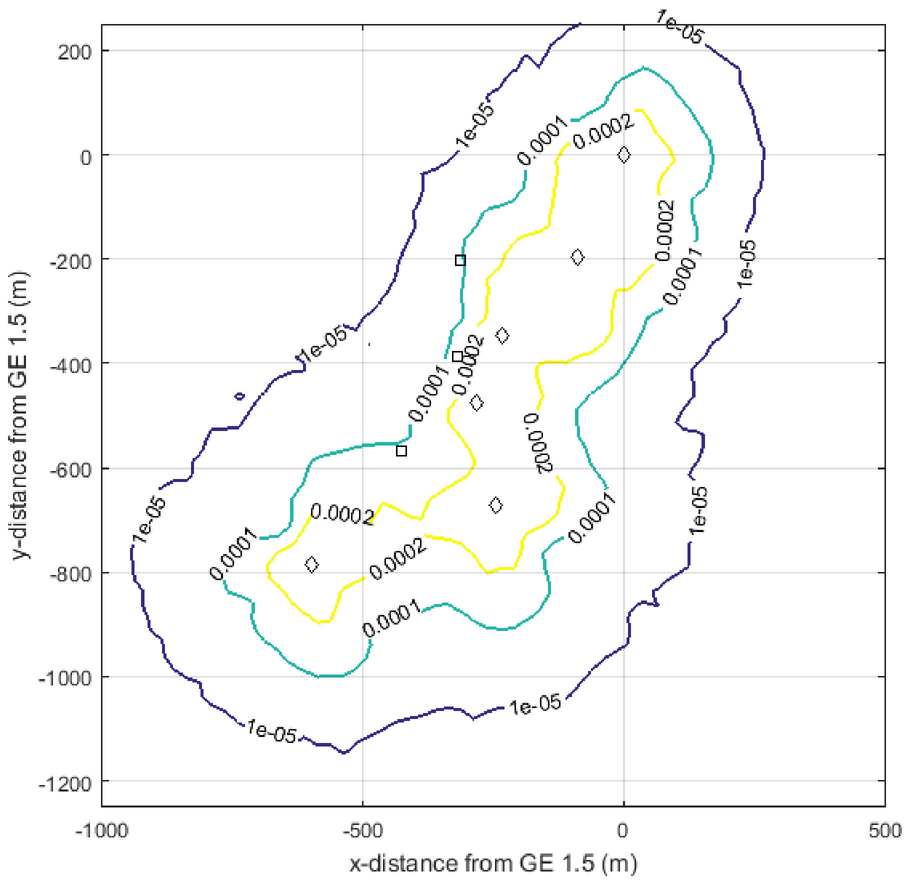


**FIGURE 7** Probability of impact for sheds (□). Turbines are indicated by open diamonds (◇)

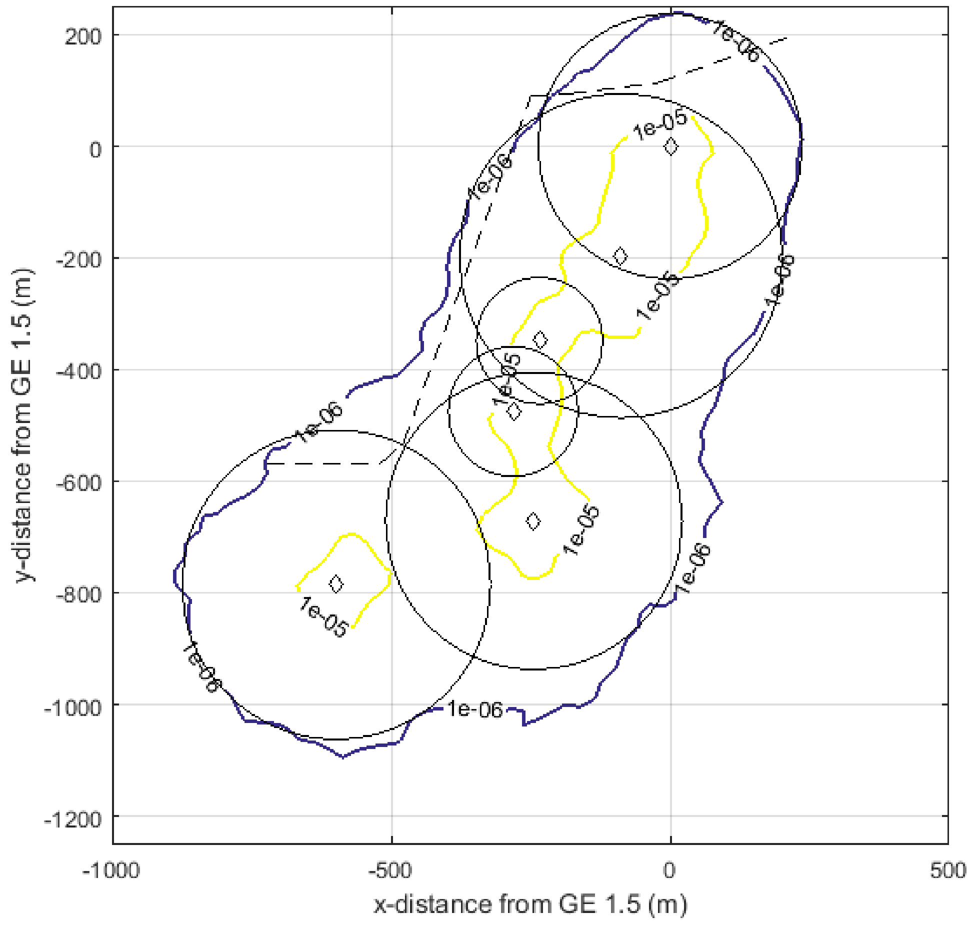


**FIGURE 8** Probability of point impact; turbines are indicated by open diamonds (◊) with circles of radius two times the overall height

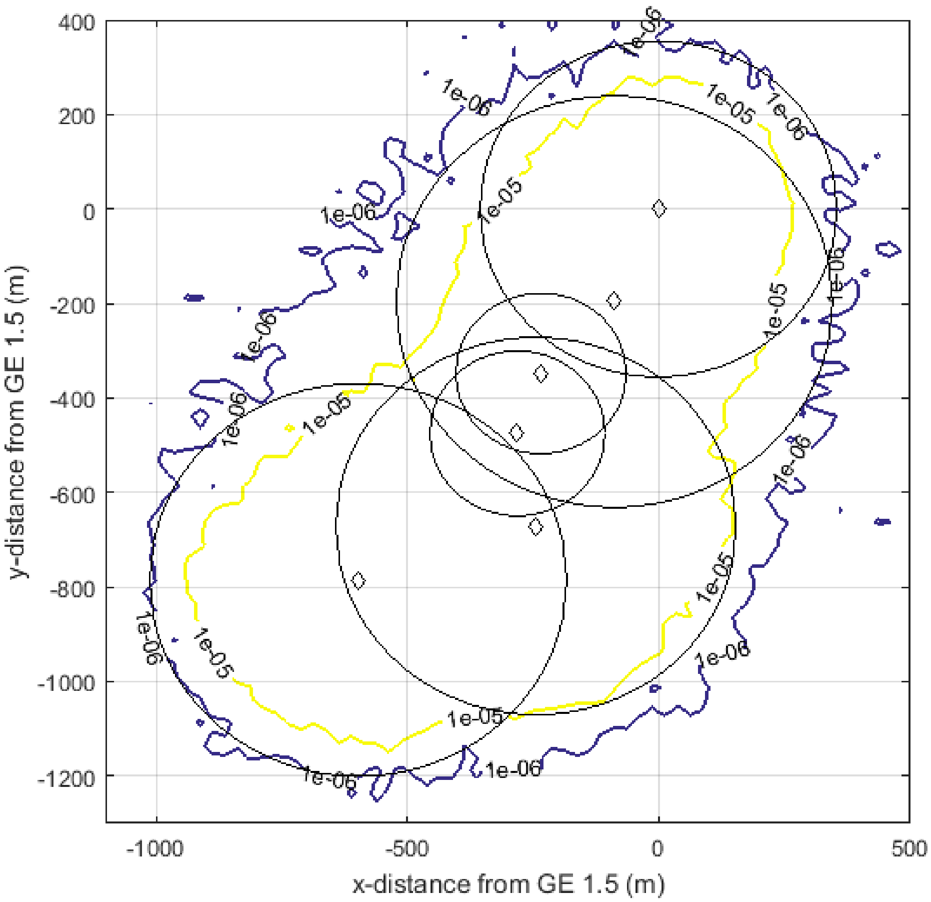


**FIGURE 9** Probability of building impact; turbines are indicated by open diamonds (◊) with circles of radius three times the overall height